Available online at www.sciencedirect.com
ScienceDirect
Earth and Planetary Science Letters 263 (2007) 32–44
EPSL
www.elsevier.com/locate/epsl

Ediacaran growth of the marine sulfate reservoir

Galen P. Halverson [a,*], Matthew T. Hurtgen [b]

[a] Geology & Geophysics, School of Earth & Environmental Sciences, University of Adelaide, SA 5005, Australia
[b] Department of Earth and Planetary Sciences, Northwestern University, 1850 Campus Dr., Evanston, IL 60208, USA

Received 20 March 2007; received in revised form 10 August 2007; accepted 15 August 2007
Available online 31 August 2007
Editor: M.L. Delaney

Abstract

The sulfur isotope record as preserved in sedimentary sulfate and sulfide minerals reflects the progressive oxidation of Earth's surface environment. The latest Proterozoic to early Paleozoic marine sulfur isotope record is distinguished by unusually high $\delta^{34}S$ values in marine sulfates and sulfides. Geological considerations and sulfur-isotopic data indicate that the ^{34}S-enrichment of the marine sulfate reservoir was the result of a rapid increase in the net fractionation between sedimentary sulfate and pyrite (Δ^{34}S) without a compensatory decline in the fractional burial rate of pyrite (f_{pyr}). A simple one-box model, in which Δ^{34}S is linked non-linearly to marine [SO_4], is used to explore the response in sedimentary sulfur isotope records ($\delta^{34}S_{sulf}$ and $\delta^{34}S_{pyr}$) to an increasing marine sulfate reservoir. The model results, when compared with a compilation of existing $\delta^{34}S_{sulf}$ and $\delta^{34}S_{pyr}$ data, suggest that the marine sulfate reservoir grew rapidly to roughly Phanerozoic levels in the middle Ediacaran Period, before the Gaskiers glaciation and prior to the onset of the Shuram–Wonoka negative δ^{13}C anomaly. It is further hypothesized that pO_2 levels rose prior to the onset of this extreme perturbation to the global carbon cycle, permitting the oxidation of a previously euxinic deep ocean and appearance of the first Ediacaran fauna by ca. 575 Ma, despite the enormous demand on oxidants implied by this large magnitude and long duration carbon isotope anomaly.

Keywords: sulfate; sulfur isotopes; Neoproterozoic; oxygen; carbon isotopes

1. Introduction

The Precambrian–Cambrian boundary (ca. 542 Ma) marks the most profound transition of the surface environment in Earth's history. The appearance of the macroscopic metazoa just before the close of the Precambrian and their rapid radiation and ecological expansion in the early Phanerozoic were likely consequences of an increase in atmospheric oxygen concentrations to roughly modern levels (Knoll, 2003). In turn, the metazoa dramatically impacted the global carbon cycle. The development of larger organisms and higher trophic levels altered the packaging and processing of organic matter (Logan et al., 1995), while the advent of calcareous biocalcification expanded the range of carbonate precipitation and decreased the carbonate saturation of seawater (Ridgwell and Zeebe, 2005). Not coincidentally, the interval spanning the Precambrian–Cambrian boundary (PCB) also figured as a key transition in the evolution of the marine sulfur cycle, related to the progressive oxidation of the oceans (Canfield and Teske, 1996).

* Corresponding author. Tel.: +61 8 8303 5378; fax: +61 8 8303 4347.
E-mail address: galen.halverson@adelaide.edu.au (G.P. Halverson).

0012-821X/$ - see front matter © 2007 Elsevier B.V. All rights reserved.
doi:10.1016/j.epsl.2007.08.022

This change is manifested in a marked increase in the average isotopic fractionation between contemporaneous sedimentary sulfate and sulfide ($\Delta^{34}S$), which presumably records an increase in sulfate availability as a consequence of increasing oxygenation of the ocean-atmosphere system (Canfield and Teske, 1996; Hurtgen et al., 2005; Fike et al., 2006).

A prominent feature of the late Neoproterozoic to Paleozoic sulfur isotope record is a peak in the $\delta^{34}S$ of seawater sulfate ($\delta^{34}S_{sulf}$) at values of 30 to 40‰ spanning the PCB (e.g. Holser and Kaplan, 1966; Claypool et al., 1980; Kampschulte and Strauss, 2004) (Fig. 1). $\delta^{34}S$ values then decline gradually through the remainder of the Paleozoic. The long time scale of this anomaly (Fig. 1) precludes models invoking ocean overturn or similar mechanisms (e.g. Holser, 1977; Strauss et al., 2001), which would generate only short-term perturbations.

Assuming that the $\delta^{34}S_{sulf}$ data roughly represents the evolution of the whole ocean sulfate reservoir, a conventional view to account for the high values is that they record increases in the fractional amount of sulfur buried as pyrite (f_{pyr})(e.g. Kampschulte and Strauss, 2004). But, whereas declining f_{pyr} may have contributed to declining $\delta^{34}S_{sulf}$ in the Paleozoic, it is hard to envision first increasing then sustained high f_{pyr} at a time of widespread oxygenation of the marine environment. Alternatively, the high $\delta^{34}S_{sulf}$ values at the PCB can be explained by high net fractionation between seawater sulfate and pyrite (Shields et al., 1999). Yet while increasing $\Delta^{34}S$ across the PCB is substantiated by the sulfur isotope record (Canfield and Teske, 1996; Schröder et al., 2004; Hurtgen et al., 2005; Fike et al., 2006), there is no reason to believe or data to support a substantial decrease in $\Delta^{34}S$ over the next several hundred million years, as would be required to account for declining $\delta^{34}S_{sulf}$ beginning in the Ordovician (Fig. 1).

Here we employ a simple one-box model to simulate the effects of an Ediacaran (635–542 Ma) increase in marine sulfate concentration on the sedimentary sulfur isotope record. Model results suggest that the peak in $\delta^{34}S_{sulf}$ spanning the PRB can be understood as a direct consequence of dramatic growth in the marine sulfate reservoir to roughly modern levels sometime in the middle Ediacaran period, itself a likely result of a contemporaneous oxygenation event (Canfield, 2005; Catling and Claire, 2005). Furthermore, the model results, when compared with a compilation of Ediacaran sulfur isotope data, suggests that the oxygenation event occurred prior to, rather than after, the large Shuram–Wonoka negative $\delta^{13}C$ anomaly (e.g. Le Guerroué et al., 2006) that punctuates the middle–late Ediacaran Period.

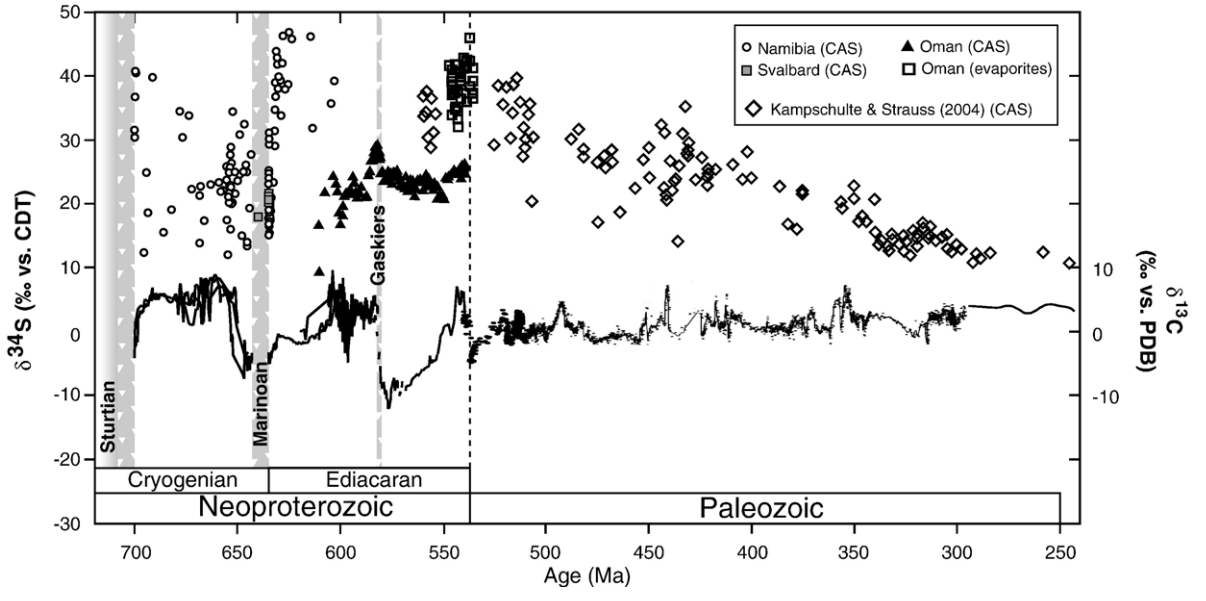

Fig. 1. A composite $\delta^{34}S_{sulf}$ record and accompanying $\delta^{13}C_{carb}$ record for the Neoproterozoic and Phanerozoic. Neoproterozoic $\Delta^{34}S$ data are from carbonate-associated sulfate (CAS) (Hurtgen et al., 2002, 2004, 2006; Fike et al., 2006, and this paper) and evaporite data (across the PCB; Schröder et al., 2004). Phanerozoic CAS data are from Kampschulte and Strauss (2004). This compilation omits many of the available data from the interval spanning the Precambrian–Cambrian Boundary (PCB) due to poor age constraints on many of these data. Nevertheless, the gross pattern of high $\delta^{34}S_{sulf}$ beginning in the late Neoproterozoic followed by a long-term decrease in the Paleozoic is clear. The carbon isotope compilation for marine carbonates is derived from previous compilations for the Neoproterozoic (Halverson et al., 2005; Halverson, 2006) and the Paleozoic (Derry et al., 1994; Hayes et al., 1999; Saltzman, 2005). The age for the end of the so-called Marinoan glaciation is from Condon et al. (2005).

2. New sulfur isotope data

2.1. Methods

Carbonate-associated sulfate (CAS) was extracted from carbonate rocks using a method modified slightly from Burdett et al. (1989) and described in more detail in Hurtgen et al. (2006). Pyrite was extracted from the insoluble residue using the chromium reduction method (Canfield et al., 1986). Sulfur isotope ratios, expressed as per mil (‰) deviations versus V-CDT, were determined at Indiana University. For both sulfate and sulfide analyses, approximately 0.5 mg of sample (either $BaSO_4$ or Ag_2S) was mixed with excess V_2O_5 (2 to 3 mg) and combusted in an Elemental Analyzer connected to a Finnigan MAT 252 gas source isotope ratio mass spectrometer. Repeat analysis of standards indicates a typical precision of ± 0.2‰.

2.2. Results

We analyzed sixteen new samples from the platform facies of the Elandshoek Formation in the lower Ediacaran Tsumeb Subgroup and its foreslope facies equivalent (Karibib Formation)(Table 1). These data represent a continuation up section of a large set of sulfur isotope data acquired from the underlying Maieberg Formation (Hurtgen et al., 2006) and were intended to test whether or not the very high (>40‰) $\delta^{34}S$ values characteristic of the upper Maieberg Formation continued. Indeed, the Elandshoek and middle Karibib data (Table 2.2) are similarly ^{34}S-enriched (31.5 to 47.0‰) and show no indication of a decrease to the more normal (21–29‰) values that characterize the presumably somewhat younger (Halverson et al., 2005) Khufai Formation in Oman (Fike et al., 2006). Nor is any strong $\Delta^{34}S$ gradient between inner and outer shelf indicated, as was the case during deposition of the middle Maieberg Formation. Only four of the samples, all deposited on the foreslope, contained sufficient amounts of pyrite for sulfur isotope analysis ($\delta^{34}S_{pyr}$=−2.9 to 44.2‰). The combination of these new data and the recently published data from Oman (Fike et al., 2006) suggest a decline in $\delta^{34}S^{34}S_{sulf}$ of >20‰ sometime in the early Ediacaran Period, at approximately the same time that marine $\delta^{13}C$ returned to positive values following the postglacial negative anomaly (Fig. 1) (Table 1).

3. The $\delta^{34}S_{sulf}$ record

The anomalously high $\delta^{34}S_{sulf}$ values spanning the PCB (Fig. 1) have been recognized for decades based on data from marine evaporites (Holser and Kaplan, 1966; Pisarchik et al., 1977; Holser, 1977; Claypool et al., 1980; Strauss, 1993; Schröder et al., 2004). More recently acquired $\delta^{34}S_{sulf}$ data from barite, phosphate, and carbonate-associated sulfate (CAS) agree well with the older evaporite data (Wang and Chu, 1991; Shields et al., 1999, 2004; Kampschulte and Strauss, 2004; Goldberg et al., 2005). The general pattern established by evaporite data is paralleled by sedimentary sulfides (Ross et al., 1995; Strauss, 1997), even though these are not a direct proxy for seawater $\delta^{34}S$. Fig. 1 shows a compilation of evaporite data from the PCB interval (Schröder et al., 2004) with published and new $\delta^{34}S_{CAS}$ data from the middle and late Neoproterozoic (Hurtgen et al., 2002, 2004, 2005, 2006; Fike et al., 2006) to the end of the Paleozoic (Kampschulte and Strauss, 2004).

Table 1
New sulfur isotope data from the lower Ediacaran, platformal Tsumeb Subgroup and its foreslope equivalent Karibib Formation, northern Namibia

Strat. height (m)	Formation	Facies	$\delta^{34}S_{sulf}$	$\delta^{34}S_{pyr}$	$\delta^{13}C$
578	Elandshoek	Platform	45.9	No pyrite	−1.54
551	Elandshoek	Platform	47.0	No pyrite	−1.60
488	Elandshoek	Platform	46.4	No pyrite	−1.37
470	Elandshoek	Platform	33.9	No pyrite	−0.95
434	Elandshoek	Platform	41.9	No pyrite	−0.22
398	Elandshoek	Platform	36.9	No pyrite	−0.74
380	Maieberg	Platform	41.9	No pyrite	−1.03
362	Maieberg	Platform	34.8	No pyrite	−1.72
326	Maieberg	Platform	31.5	No pyrite	−2.93
335	Karibib	Foreslope	39.8	44.16	3.23
325	Karibib	Foreslope	36.4	No pyrite	6.09
287.1	Karibib	Foreslope	32.6	No pyrite	0.62
277.1	Karibib	Foreslope	46.6	No pyrite	0.75
267.9	Karibib	Foreslope	No CAS	26.9	2.68
256.8	Karibib	Foreslope	No CAS	−2.9	0.59
246	Karibib	Foreslope	No CAS	28.1	0.52

Stratigraphic height is from the base of the Tsumeb Subgroup (Elandhsoek and Maieberg Fms.) and Karibib Formation. ä^{13}C data from Halverson et al. (2005).

The $\delta^{34}S_{sulf}$ compilation for the Neoproterozoic used here is tied directly to the $\delta^{13}C$ curve, which is modified from (Halverson, 2006). We do not attempt to incorporate all available $\delta^{34}S_{sulf}$ data for the interval of interest (635–250 Ma) since poor age constraints prevent precise correlations, and a more extensive compilation could impose artificial variability in the record, particularly for the Neoproterozoic. Indeed, correlating separate Neoproterozoic successions is challenging due to the enduring controversy over the ages of glaciations and $\delta^{13}C$ anomalies. The rationale for the correlations underlying this compilation are discussed in detail in Halverson et al. (in press), and while they are prone to change pending new age constraints, the broad trends in the Ediacaran–Paleozoic record, which are of interest here, are not likely to be significantly modified (Fig. 1).

The most complete $\delta^{34}S_{sulf}$ record for this time interval is from the Ediacaran of Oman (Schröder et al., 2004; Fike et al., 2006). While this record cannot be tied unambiguously to the immediately post-Marinoan (i.e. 635 Ma; Hoffmann et al., 2004; Condon et al., 2005) data from Namibia and poor radiometric age control preclude precise calibration of the record, the pattern in $\delta^{34}S_{sulf}$ for the Ediacaran is evident. Unusually high $\delta^{34}S_{sulf}$ values (30–40‰) characterize both the beginning and end of the Ediacaran period, while values closer to 20‰ prevail through the middle of the period. The Paleozoic Era is distinguished by a long-term decline in $\delta^{34}S_{sulf}$ from the PCB peak towards unusually low $\delta^{34}S_{sulf}$ values (as low as 10‰) in the late Permian (Newton et al., 2004; Kampschulte and Strauss, 2004), punctuated by many higher order fluctuations (Fig. 1).

4. The Neoproterozoic sulfur cycle

In the modern ocean, the concentration of sulfate is 28 mM and the residence time is 10 to 20 m.y. (Holser et al., 1989). In steady state, the sulfur-isotopic composition of that sulfate, which today is 21‰, is governed by the net isotopic fractionation between seawater sulfate and sedimentary sulfide ($\Delta^{34}S$), largely imparted by bacterial sulfate reduction (BSR), and the fraction of total sulfur buried as sulfide (f_{pyr}). The long residence time of sulfate in the Cenozoic ocean has buffered it against large shifts in $\delta^{34}S_{sulf}$ (Paytan et al., 1998). The marine sulfate concentration was likely much lower in much of the Neoproterozoic, as evinced by the large variability in the $\delta^{34}S_{sulf}$ record of CAS (Hurtgen et al., 2002) and similarity in average $\delta^{34}S_{sulf}$ and $\delta^{34}S_{pyr}$ values (Canfield, 2004) in middle Neoproterozoic rocks. However, sulfate concentrations apparently reached sufficient levels (at least temporarily) to allow widespread deposition of bedded evaporites to be deposited at ca. 800 Ma (Grotzinger and Kasting, 1993).

The PCB $\delta^{34}S_{sulf}$ excursion is not the only prominent anomaly in the Neoproterozoic sulfur isotope record. Two salient spikes in $\delta^{34}S_{sulf}$ are preserved in the cap carbonates to the Cryogenian glaciations (Fig. 1). However, these positive spikes differ from the PCB anomaly in that they appear to be directly related to the end of glacial episodes, were likely not nearly as long-lived (<20 m.y.), and were facilitated by very low sulfate concentrations (Hurtgen et al., 2002). Furthermore, at least in the case of the post-Marinoan (635 Ma) anomaly (Hurtgen et al., 2006), the positive $\delta^{34}S_{sulf}$ signal may be attributed solely to a restricted surface water reservoir rather than a whole ocean signal (Holser, 1977). Indeed, significant differences (>20‰) in time-equivalent units from different environments in overlying rocks (Hurtgen et al., 2006) suggest a stratified water column with isotopically distinct sulfur reservoirs. These large coeval differences in $\delta^{34}S_{sulf}$, coupled with short-term changes in $\delta^{34}S_{sulf}$ of up to 10‰ in the cap dolostone directly overlying the Marinoan glaciation, imply that marine sulfate concentrations were extremely low (<1 mM) following glaciation (635 Ma; Hoffmann et al., 2004; Condon et al., 2005). Judging from the absence of evaporites in post-Marinoan cap carbonate sequences and their prevalence in sediments straddling the PCB in northeastern Gondwana (e.g. Oman; Schröder et al., 2003), it appears that the marine sulfate reservoir must have grown rapidly to near modern levels by the latter half of the Ediacaran Period. This hypothesis is corroborated by increasing CAS concentrations in middle Ediacaran carbonates (Fike et al., 2006; Kaufman et al., 2007), as well as data from fluid inclusions in the Ara Salt of Oman, which indicate $[SO_4] \geq 23$ mM at the PCB (Horita et al., 2002).

In addition to a dramatic rise in marine $[SO_4]$, the late Neoproterozoic–early Paleozoic witnessed an increase in average $\Delta^{34}S$ (Ross et al., 1995), most likely related to a rise in atmospheric O_2 (Canfield and Teske, 1996; Canfield, 1998, 2004). Whereas the increase in $\Delta^{34}S$ had been interpreted to record the innovation of sulfur disproportionation reactions by newly evolved non-photosynthetic sulfur oxidizing bacteria (Canfield and Teske, 1996), it appears that disproportionation reactions were occurring as early as 1.3 Ga (Johnston et al., 2005). Low $\Delta^{34}S$ values during the Meso-early Neoproterozoic were liked maintained, in part, by efficient burial of sulfur as sedimentary sulfide due to low oxygen concentrations (Hurtgen et al., 2005). The large Neoproterozoic increase in $\Delta^{34}S$ identified by Canfield and Teske (1996) now appears to have occurred some

time in the Ediacaran Period (Hurtgen et al., 2005; Fike et al., 2006). Thus, the rise in $\Delta^{34}S$ broadly paralleled the growth of the marine sulfate reservoir. At the same time, the continental surface sulfur reservoir was also growing as a result of increased evaporite deposition and a shift in sulfide burial from the deep ocean to continental margins (Ross et al., 1995; Canfield, 2004), where it was more likely to be subaerially exposed by fluctuations in sea level or tectonic uplift.

The linkage in the geological record between a rise in $[SO_4]$ and $\Delta^{34}S$ is not surprising since both are in part a function of pO_2: the former through oxidative weathering of pyrite and the latter through increased sulfur disproportionation and decreased burial efficiency of sulfide. Empirical evidence demonstrates that the fractionation between sulfate and sulfide observed during BSR is controlled, in large part, by $[SO_4]$ (Habicht et al., 2002). The net fractionation between sulfate and sulfide is further amplified by the availability of O_2, which drives the oxidative portion of the marine sulfur cycle and generates additional fractionation via disproportionation reactions (Canfield and Teske, 1996).

It follows that increasing pO_2 and $[SO_4]$ caused f_{pyr} to decrease through increased evaporite deposition and decreased burial efficiency of pyrite due to increased re-oxidation of sulfide in porewaters and the water column. However, based on the sulfur isotope record (Canfield, 2004) and modeling of sulfur fluxes in the Paleozoic (Berner, 2004), f_{pyr} continued to decrease throughout the Paleozoic, and was thus probably controlled by additional factors, such as the availability of Ca^{2+} (for evaporite precipitation), reactive Fe (for pyrite deposition) and labile organic matter (for BSR).

5. Model parameters and constraints

To model the evolution of $\delta^{34}S_{sulf}$ during the Ediacaran Period (635 to 542 Ma), we employ a simple box model (Fig. 2a) with a single box representing the marine sulfate reservoir with mass M_{sulf}. The model is forced by imposed sulfate concentrations, which are varied via

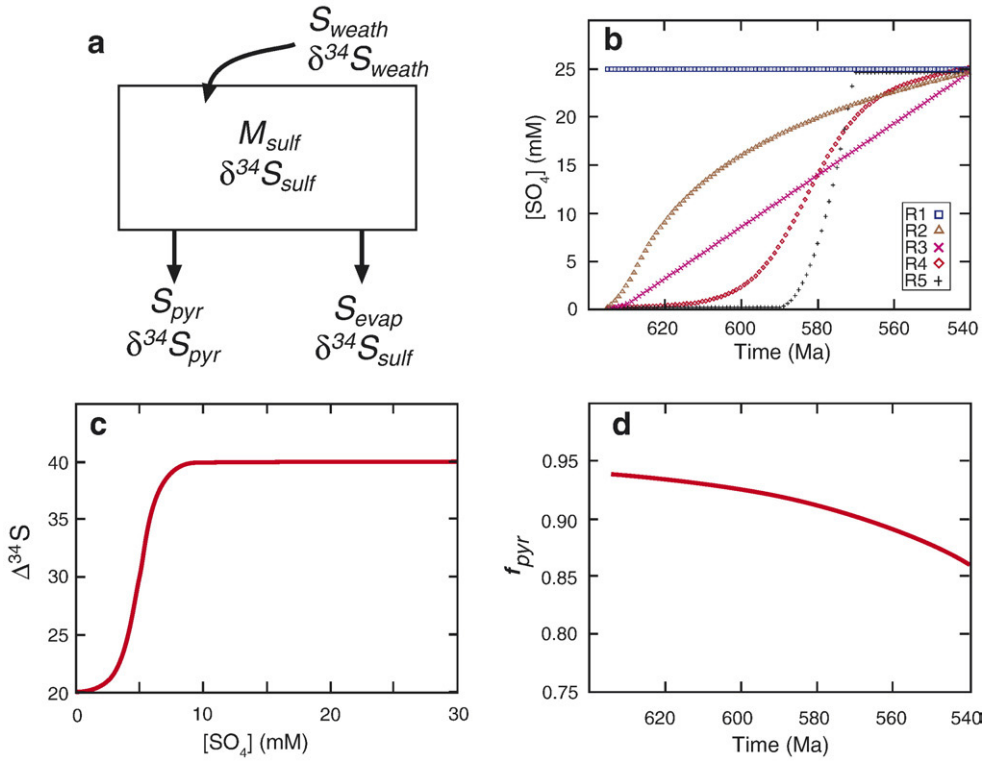

Fig. 2. Summary of the one-box sulfur isotope model and parameters used in model runs (R1–5). a. One-box sulfate reservoir model: the continental sulfate weathering flux, S_{weath}, is a combination of dissolved evaporite minerals and oxidized sulfides and has a fixed isotopic composition ($\Delta^{34}S$) of 5‰. The marine sulfate reservoir, M_{sulf}, has isotopic composition $\delta^{34}S_{sulf}$. Sulfur is removed from the ocean as sulfide (S_{pyr}) and evaporite (S_{evap}) minerals of isotopic composition $\delta^{34}S_{pyr}$ and $\delta^{34}S_{sulf}$, respectively. $\Delta^{34}S = \delta^{34}S_{sulf} - \delta^{34}S_{pyr}$ $f_{pyr} = S_{pyr}/(S_{pyr}+S_{evap})$. b. Imposed evolution of marine $[SO_4]$ in the 5 model runs. Changes in $[SO_4]$ are realized by imbalances between the sulfur input and output fluxes. c. Parameterization for $\Delta^{34}S$ as a function of $[SO_4]$ and (d.) Evolution of f_{pyr} through the Ediacaran Period as discussed in text.

imbalances between the sulfate input and output from the marine sulfate reservoir. Sulfate input to the ocean, S_{weath}, is derived from continental weathering (sulfides + evaporites) and has isotopic composition $\delta^{34}S_{weath}$. Sulfur is removed as pyrite (S_{pyr}), with isotopic composition $\delta^{34}S_{pyr}$ and as sulfate evaporates (S_{evap}) with the same isotopic composition as marine sulfate. $\Delta^{34}S$ equals the average net difference between $\delta^{34}S_{sulf}$ and $\delta^{34}S_{pyr}$, while the fraction of sulfur removed as sulfide, f_{pyr} = pyrite/(pyrite + sulfate). Sulfur exchange with the oceanic crust is neglected since little fractionation is associated with anhydrite incorporation into basalt, and because over time scales of 10s of millions of years, the loss of sulfate into mid-ocean ridges is balanced by the gain of sulfate via off-axis dissolution (Alt, 1995).

5.1. Marine sulfate concentration and continental weathering flux

Sulfur isotope data from the lower Maieberg Formation cap carbonate sequence in Namibia suggest that sulfate concentrations in the post-Marinoan (635 Ma) ocean were very low (Hurtgen et al., 2006). In order to quantify in a rough manner the sulfate concentrations at this time, we applied the model of Kah et al. (2004) to $\delta^{34}S_{sulf}$ variations of 10‰ recorded in the Keilberg cap dolostone at the base of the cap carbonate sequence (Hurtgen et al., 2006).

Although sedimentation rates for the cap dolostone are poorly constrained and controversial (Trindade et al., 2003; Hoffman et al., 2007), the fact that it was deposited entirely within the transgressive phase driven by presumably rapid (~2000 years; Hyde et al., 2000) melting of the Marinoan ice sheets suggests a time scale for the $\delta^{34}S_{sulf}$ shifts (which do not occupy the entire cap dolostone) of less than 10,000 years. Assuming a conservative time scale of 10,000 years for the calculation yields a $[SO_4]$ of ~60 μM. This figure can only be regarded as an approximate maximum value for whole ocean concentration since the cap dolostone is interpreted to have been deposited from a stratified surface ocean reservoir (Hurtgen et al., 2006), and the calculation is based on assumptions (i.e. the value of f_{pyr}) that are likely not valid for the post-glacial ocean. Notwithstanding the uncertainty, it is clear that $[SO_4]$ at 635 Ma was extremely low and surely less than 1% of the modern value of 29 mM. In all model runs, except the control (R1), initial $[SO_4]$ is set at 0.25 mM.

If we assume that the predominant source of sulfate to the oceans is the oxidative weathering of pyrite on the continents, then growth of the sulfate reservoir can only be achieved when $S_{weath} > S_{pyr} + S_{evap}$. This non-steady state situation may have been the natural response to a gradually increasing continental sulfur reservoir (i.e. sulfide and sulfate minerals stored in sedimentary rocks on the margins of the cratons; Canfield, 2004) coupled with increased rates of pyrite oxidation due to elevated pO_2.

In the control run, R1, S_{weath} is set at the approximate average Phanerozoic rate of 1×10^{14} g S yr^{-1} (Berner, 2004), and $[SO_4]$ is fixed at 25 mM. In the remaining runs, the model sulfate reservoir is allowed to grow via an imposed imbalance in the input and output fluxes, starting from the end of the Marinoan glaciation at 635 Ma. S_{weath} is set in runs R2–5 to increase from $\sim 10^{12}$ g S yr^{-1} towards $\sim 10^{14}$ g S yr^{-1} (approximately the modern flux; Berner, 2001). S_{burial} is set to increase in a parallel fashion to S_{weath}, but is offset in such a manner as to achieve the desired pattern of growth in the marine sulfate reservoir (Fig. 2b) without imposing unreasonable residence times for sulfate (Fig. 3a). In R2, the sulfate reservoir begins growing rapidly in the early Ediacaran Period, then the rate of growth tapers off in the latter half. In R3, $[SO_4]$ grows linearly throughout the Ediacaran Period. In R4, growth is concentrated between 600 and 565 Ma, and in R5, it increases sharply at ca. 580 Ma.

5.2. $\Delta^{34}S$ and f_{pyr}

The two most important variables governing the long term evolution of marine $\delta^{34}S_{sulf}$ are $\Delta^{34}S$ and f_{pyr}. $\Delta^{34}S$ is largely a function of sulfate concentration, which controls the fractionation entailed during BSR (Habicht et al., 2002). The availability of O_2 is also important, as it may increase the extent to which sulfide produced through BSR is oxidized to sulfur intermediates (e.g. S^0 and $S_2O_3^{2-}$), which in turn can undergo disproportionation reactions, thereby facilitating larger fractionations (Jørgensen, 1990; Canfield and Thamdrup, 1994; Habicht and Canfield, 2001). Coupled sulfate and pyrite data from the latest Ediacaran to early Cambrian Ara Formation (Amthor et al., 2003) in Oman preserve an average $\Delta^{34}S$ of ~38‰ (Schröder et al., 2004). A recently published high resolution data set of $\Delta^{34}S_{CAS}$ and $\Delta^{34}S_{pyr}$ data from Oman (Fike et al., 2006) similarly indicates an increase in $\Delta^{34}S$ in the middle Ediacaran period (Fig. 3b). These data appear to corroborate pyrite data from early Paleozoic rocks (Canfield and Teske, 1996) that suggest that $\Delta^{34}S$ reached typical Phanerozoic values by the beginning of the Paleozoic.

Here, we parameterize $\Delta^{34}S$ as a direct function of $[SO_4]$ (Fig. 2c). The minimum $\Delta^{34}S$ is set to 20‰, based on isotopic data from the cap dolostone to the Marinoan

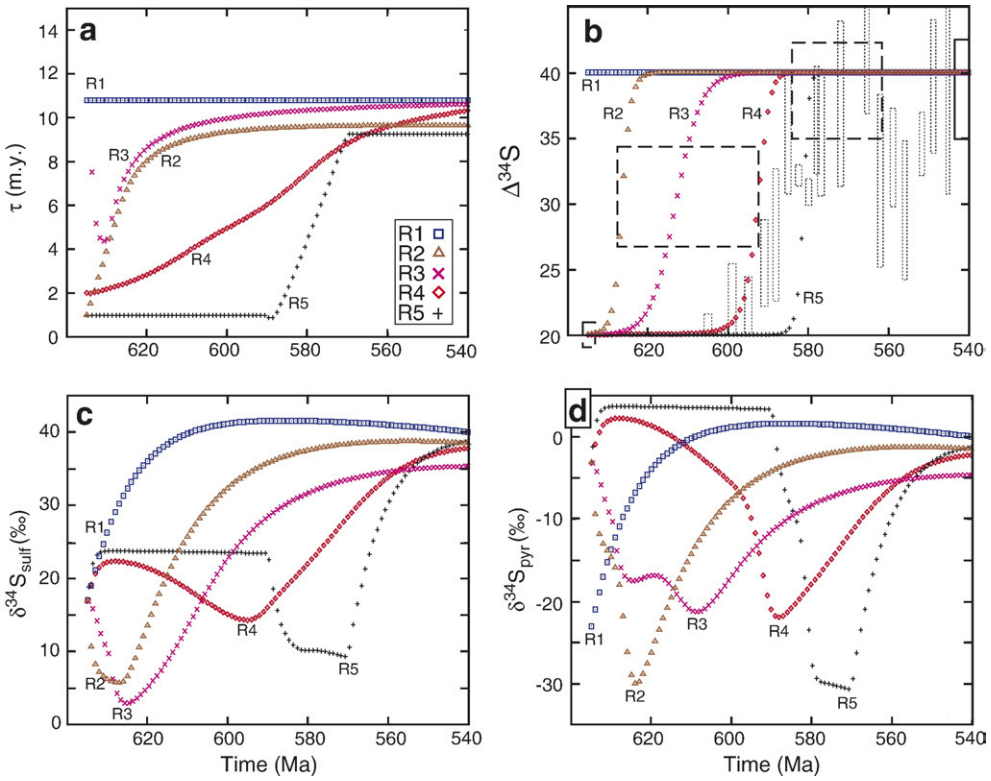

Fig. 3. Model results for runs R1–R5 plotted as a function of time, from 635–540 Ma. a. Residence time (calculated using the weathering flux), which is tracked to show that the model results are not unduly affected by large disparities in weathering flux relative to the sulfate reservoir. b. $\Delta^{34}S$, which in R2–R5 increases rapidly from 20 to 40‰ as [SO_4] increases from 1 to 10 mM (Fig. 2c). Boxes show approximate constraints on average $\Delta^{34}S$ from coupled sulfide and sulfate data: solid lines, from Schröder et al. (2004); dashed lines, from Hurtgen et al. (2005); and dotted lines from Fike et al. (2006). c. $\delta^{34}S$ value of the marine sulfate reservoir, and by implication, of sedimentary sulfate (CAS, evaporite minerals, and phosphate). d. The average $\Delta^{34}S$ composition of sedimentary sulfide, calculated by substracting $\Delta^{34}S$ from $\delta^{34}S_{sulf}$. Integrations were performed every 100 k.y.

glaciation (Hurtgen et al., 2005) and isotopic data from the Mesoproterozoic, which suggest an average, net $\Delta^{34}S$ of ~20‰ (Canfield, 1998) even at times when sulfate concentrations are deemed very low (0–10% modern values: Kah et al., 2004). Maximum $\Delta^{34}S$ is set to 40‰, which is the approximate value obtained from the PCB interval in Oman (Schröder et al., 2004) and is close to the average value for the Paleozoic (Petsch and Berner, 1998; Berner, 2004). $\Delta^{34}S$ is set to increase sharply from 20 to 40‰ between 0 and 10 mM SO_4 (Fig. 2c), the same range over which ^{34}S-fractionation by bacterial sulfate reducers increases virtually stepwise from <6‰ to 440‰ (Habicht et al., 2002).

f_{pyr} is commonly calculated from $\delta^{34}S_{sulf}$ data, assuming steady state conditions and a constant $\Delta^{34}S$. However, since the objective of this paper is to model $\delta^{34}S_{sulf}$ values, we cannot calculate f_{pyr} in this manner. Given the low sulfate concentrations following the Marinoan glaciation (Hurtgen et al., 2006), it seems reasonable to presume that virtually all marine sulfur was buried as pyrite and that f_{pyr} was close to 1 in the late Neoproterozoic, as suggested by Canfield (2004). Modeled sulfur fluxes for the Phanerozoic (Berner, 2004) suggest that f_{pyr} was still relatively high at the beginning of the Cambrian, after which it generally decreased through the remainder of the Paleozoic. We allow f_{pyr} to decrease gradually from 0.94 at the beginning of the Ediacaran period (Fig. 2d), with the rate of decrease increasing towards the end of the Ediacaran, a time when increased oxygenation of bottom waters (Canfield et al., 2007) should have decreased the burial efficiency of sedimentary pyrite (Hurtgen et al., 2005).

5.3. Model results

In all model runs, $\delta^{34}S_{sulf}$ reaches values >35‰ by the close of the Ediacaran Period as a result of high $\Delta^{34}S$ and f_{pyr} values. To a first order, the differences in the timing and pattern of the rise in $\delta^{34}S_{sulf}$ are a function of the imposed timing and rate of growth of M_{sulf} (Fig. 2b) and the resulting evolution of $\Delta^{34}S$ (Fig. 3b). In control run R1 where [SO_4] concentrations are held constant at

25 mM, the rise in $\delta^{34}S_{sulf}$ from the initial value of 17‰ to ~44‰ simply records the transient as the sulfate reservoir evolves to isotopic steady state (Fig. 3c). In R2–R5, a pronounced decline in $\delta^{34}S_{sulf}$ precedes the rise and records the initial interval of rapid increase in $[SO_4]$, during which time the excess in weathering flux of relatively light sulfur (5‰) to M_{sulf} overwhelms the effect of removal of ^{34}S-depleted sulfur, while $\Delta^{34}S$ remains relatively low. Consequently, $\delta^{34}S_{sulf}$ in the early Ediacaran is highly sensitive to the rate of increase in $[SO_4]$ from 0 to <10 mM, such that in runs R4 and R5, $\delta^{34}S_{sulf}$ actually increases in the first few million years after the glaciation, compared to substantial decreases (<11‰) in runs R2 and R3. In R4 and R5, $\delta^{34}S_{sulf}$ subsequently declines as $[SO_4]$ approaches 10 mM (Fig. 3c). The decline in $\delta^{34}S_{sulf}$ in R4 is protracted over <30 m.y., compared to 410 m.y. for R5 as a result of a much slower initial rate of increase in $[SO_4]$ in the former run. Thus, insofar as growth in the marine sulfate reservoir is accomplished via addition of relatively isotopically light S from continental weathering, then the timing and magnitude of the decline in marine $\delta^{34}S_{sulf}$ reflect the timing and tempo of growth in the marine sulfate reservoir.

Additional constraints on the growth of the sulfate reservoir may be derived from the sedimentary pyrite record (Fig. 3d). In runs R4 and R5, $\delta^{34}S_{pyr}$ actually increases its values to >0‰ in the early Ediacaran, whereas it decreases to <−15‰ in runs R2 and to −3‰ in R3, where $[SO_4]$ increases rapidly after glaciation. Like $\delta^{34}S_{sulf}$, the magnitude and duration of the negative $\delta^{34}S_{pyr}$ excursion is a function of the rate at which $[SO_4]$ increases, as is the phase lag between the negative $\delta^{34}S_{sulf}$ and $\delta^{34}S_{pyr}$ spikes. Thus, in the case of R5, where

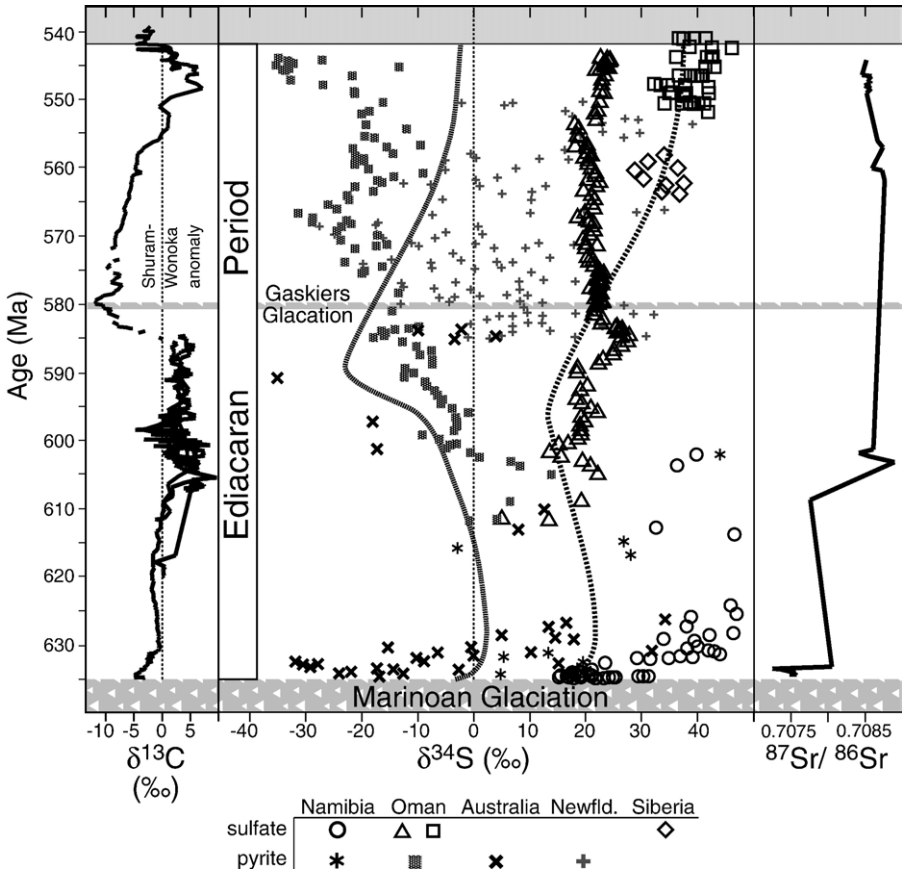

Fig. 4. Compilation of $\delta^{13}C$ (carbonate), $\delta^{34}S_{pyr}$, $\delta^{34}S_{sulf}$, and $^{87}Sr/^{86}Sr$ data for the Ediacaran Period. The pyrite record includes data from central and South Australia (Gorjan et al., 2000), the Tsumeb Subgroup and Karibib Formation in Namibia (Hurtgen et al., 2005, 2006, this paper), the Nafun Group, Oman (Fike et al., 2006), and the Conception and St. John's groups, Newfoundland (Canfield et al., 2007). The time scale for the South Australian data is based on Hurtgen et al. (2005), and the time scale for the Newfoundland data is taken directly from Canfield et al. (2007). The sulfate and carbonate records are from Fig. 1. Dashed lines are the model results for $\delta^{34}S_{pyr}$ (left) and $\delta^{34}S_{sulf}$ (right) from run R4. The strontium isotope curve, on the right, is modified from Halverson et al. (in press), with new data from Pokrovskii et al. (2006).

[SO_4] rises from 1 to 10 mM in less than 5 m.y., the anomalies are virtually in phase (Fig. 3c,d). In contrast, in R3, where the same increase occurs over 40 m.y., the nadir in $\delta^{34}S_{pyr}$ lags that of $\delta^{34}S_{sulf}$ by 10–20 m.y.

6. Discussion

High $\delta^{34}S_{sulf}$ values are achieved by the latest Ediacaran in all model runs simply because $\Delta^{34}S$ in all cases overcompensates for the gradual decline in f_{pyr}. The reason for this decoupling between two important parameters governing the $\delta^{34}S_{sulf}$ composition of the ocean cannot be addressed with our simple box model, but is important to understanding the evolution of late Neoproterozoic ocean chemistry.

Such a disconnect between these two parameters might in fact be a logical outcome of the gradual oxidation of a previously euxinic global ocean. It has been proposed (Canfield, 1998) and supported by various lines of reasoning and geochemical data (Anbar and Knoll, 2002; Shen et al., 2003; Arnold et al., 2004) that a euxinic deep ocean persisted from the late Paleoproterozoic to at least the mid-Neoproterozoic (~1.8 to <0.8 Ga). Hurtgen et al. (2006) argued that deep ocean euxinia also prevailed in the aftermath of the Marinoan glaciation, in the early Ediacaran Period. Presumably, the deep ocean was effectively oxygenated by the Cambrian, by which time oxygen-requiring animals (Runnegar, 1991) had inhabited the whole of the oceans. Thus, we can surmise that the deep ocean was euxinic at the onset of the Ediacaran, but was ventilated by the beginning of the Cambrian. Iron chemistry data from deep-water, Ediacaran sediments on the Avalon Peninsula of Newfoundland provide direct empirical evidence for at least localized oxygenation of the deep ocean (Canfield et al., 2007).

A useful analog for understanding sulfur cycling during this transitional period is the Black Sea, where euxinic deep waters are maintained today despite high pO_2 due to a stratified water column and high rates of BSR. High net fractionation between Black Sea sulfate and sedimentary pyrite ($\Delta^{34}S$ ~50‰, Lyons, 1997) is achieved due to a combination of high ambient sulfate concentrations, water column sulfide production and active re-oxidation of sulfide and production of sulfur intermediates in the chemocline (Neretin et al., 2003). Presumably, most sulfur in the Black Sea is removed as pyrite (and other sulfide minerals) and only a minimal fraction of total sulfur is removed as sulfate. Thus, it is predictable that sulfur cycling in an ocean with oxic surface and euxinic deep water would be characterized by high net $\Delta^{34}S$ and f_{pyr}.

6.1. Growth of the marine sulfate reservoir

Data from coupled $\delta^{34}S_{sulf}$ and $\delta^{34}S_{pyr}$ records (Fig. 3b: Schröder et al., 2004; Hurtgen et al., 2005; Fike et al., 2006) support the hypothesis that $\Delta^{34}S$ increased from ~20‰ to ~40‰ sometime in the middle Ediacaran Period (Figs. 3b, 4). However, it should be noted that single $\delta^{34}S_{sulf}$–$\Delta^{34}S_{pyr}$ pairs from a single samples, such as those comprising the high resolution Oman record (Fike et al., 2006), do not necessarily accurately reflect the mean $\Delta^{34}S$ of the global ocean since the net isotopic fractionation between sulfate and pyrite can be heavily influenced by local effects, such as sulfate availability, the relative importance of water column (syngenetic) versus diagenetic pyrite formation, sedimentation rates, substrate availability for BSR, and the abundance of reactive iron. We have therefore reconstructed the evolution in Ediacaran $\Delta^{34}S$ from the Fike et al. (2006) record by integrating $\delta^{34}S_{sulf}$– $\Delta^{34}S_{pyr}$ data over 50-m intervals and calculating the minimum and maximum $\Delta^{34}S$ values (cf. Hurtgen et al., 2005). While this method is still not ideal and cannot discriminate against unique basinal effects, it nonetheless paints a more realistic picture of the evolution of $\Delta^{34}S$.

The Oman data essentially fill in the much more sparse record from Hurtgen et al. (2005) and appear to confirm a rather rapid rise in $\Delta^{34}S$ towards 40‰ sometime in the middle Ediacaran (Fig. 3b) and beginning prior to the onset of the Shuram–Wonoka $\delta^{13}C$ anomaly ca. 580 Ma (Fig. 4). Significantly, the new $\delta^{34}S_{pyr}$ record from late Ediacaran sediments of the Avalon Peninsula, Newfoundland (Canfield et al., 2007), displays a range in values that is similar to that defined by the Oman $\delta^{34}S_{sulf}$ and $\delta^{34}S_{pyr}$ records. The spread in the $\delta^{34}S_{pyr}$ record can be used as a rough proxy for $\Delta^{34}S$ (Canfield and Teske, 1996): thus, it is significant that the Newfoundland $\delta^{34}S_{pyr}$ record begins to diverge shortly before 580 Ma (Fig. 4), further reinforcing evidence for an increase in $\Delta^{34}S$ at this time.

Insofar as our parameterization of the relationship between $\Delta^{34}S$ and marine sulfate concentrations (Fig. 2c) is broadly correct, then the sulfur isotope record should be a sensitive recorder of the timing of the growth of the marine sulfate reservoir. In addition to the highly-enriched $\delta^{34}S_{sulf}$ values that should follow growth of M_{sulf}, the model predicts an initial negative excursion in $\delta^{34}S_{sulf}$ due to the increase in the ^{34}S-depleted weathering flux (Fig. 3c). The decline in $\delta^{34}S_{sulf}$ occurs because S_{weath} initially overwhelms the increase in $\Delta^{34}S$ resulting from increased sulfate availability. Even though no large decline in $\delta^{34}S_{sulf}$ is apparent in any single CAS data set, the compilation does indicate that $\delta^{34}S_{sulf}$ dropped

from high (>35‰) values following the end of the Marinoan (pre-Ediacaran) glaciation to values as low as 10–20‰ between 615 and 600 Ma.

Our model also predicts a negative excursion in $\delta^{34}S_{pyr}$ during the interval of increasing $[SO_4]$ (Fig. 3d). This excursion is more pronounced than that of $\delta^{34}S_{sulf}$ because of the added effect of sharply increased $\Delta^{34}S$ values, which leverages $\delta^{34}S_{pyr}$ downwards. Theoretically, the magnitude of the $\delta^{34}S_{pyr}$ excursion will reflect the rate of increase in $\Delta^{34}S$, and implicitly, increase in marine $[SO_4]$. While the currently available data is insufficient to use the model as a basis for quantifying the rate of growth of the sulfate reservoir, the three most complete Ediacaran pyrite data sets – Australia (Gorjan et al., 2000), Oman (Fike et al., 2006; Kaufman et al., 2007), and Newfoundland (Canfield et al., 2007) – all display a prominent decline in $\Delta^{34}S_{pyr}$ to values below −20‰ in the middle Ediacaran (Fig. 4). The data from Oman also display an initial decline to ~−15‰, followed by a more pronounced drop to −30‰. However, as in Australia and Newfoundland, $\delta^{34}S_{pyr}$ values unmistakably decline following what our compilation shows to be a transient dip in $\delta^{34}S_{sulf}$ values. An increase in marine sulfate concentrations at this time is supported by a rise in average CAS concentrations (Fike et al., 2006) and abundance of evaporitic minerals in the lower Shuram Formation (Le Guerroué et al., 2006) in Oman. Overall, the sulfur isotope record most closely conforms with model run R4, and we conclude that $[SO_4]$ surpassed ~8 mM sometime before the onset of the Shuram–Wonoka negative $\delta^{13}C$ anomaly, roughly between 590 and 580 Ma (Fig. 4).

The Shuram–Wonoka carbon isotope anomaly was the most extreme in Earth's history (Le Guerroué et al., 2006; Fike et al., 2006). Given the extremely low $\delta^{13}C$ values and the apparent longevity that characterizes it (Fig. 4), it is inescapable to conclude that the source of the highly ^{13}C-depleted carbon responsible for this anomaly was the oxidation of organic matter or methane, or a combination of the two. Marine sulfate would have been a likely terminal electron acceptor in the oxidation of this reduced carbon reservoir, thus this extreme perturbation to the global carbon cycle should also have affected the sulfur cycle. This perturbation is recorded in a coeval spike in $\delta^{34}S_{sulf}$ recorded in both Oman (Fike et al., 2006) and Death Valley (Kaufman et al., 2007) and may also be reflected in a transient return to lower $\Delta^{34}S$ values sometime after the onset of this anomaly, as seen in the Oman data (Fig. 3b).

A notable inconsistency in the Ediacaran sulfur isotope record is the absence of a pronounced rise in $\delta^{34}S_{sulf}$ in the late Ediacaran CAS record from Oman (Fig. 4). One explanation for the offset between the Oman CAS record and other CAS and evaporite records could be that the Huqf basin was partly isolated from the global ocean and heavily influenced isotopically by local influx of ^{34}S-depleted sulfur from continental run-off. This hypothesis is speculative, but could explain why both the late Ediacaran pyrite and sulfate records in Oman are negatively offset from the model predictions and other data sets (Fig. 4), while still exhibiting a similar evolution in $\Delta^{34}S$.

6.2. Implications for late Neoproterozoic oxygenation

The sulfur isotope record suggests that growth of the marine sulfate reservoir in the middle of the Ediacaran Period was driven by increased oxidative weathering of continental sulfides. While this increase may have been facilitated by the greater abundance of easily weathered sulfides exposed during the Pan-African orogeny (Ross et al., 1995; Canfield, 2004), it must also have required that oxygen concentrations in the atmosphere surpass some critical threshold. Because this threshold is entirely unconstrained (Canfield, 2005), it is impossible at this stage to quantify how high pO_2 rose. Nevertheless, it is safe to assume that there must have been a major source of free oxygen to the surface environment at this time. The obvious source of this O_2 was the production and burial of photosynthetically-derived organic matter. Many post-glacial, early Ediacaran cap-carbonate sequences contain abundant organic matter. Thick (≥150 m) accumulations of relatively organic-rich shales occur in the Sheepbed Formation in northwest Canada, the Canyon Formation and equivalent Dracoisen Formation in East Greenland and Svalbard, respectively, the Pertataka Formation in central Australia, and the Masirah Bay Formation in Oman, the oldest commercial petroleum source bed in the world (Grantham et al., 1988). This time period coincides with a steep rise in the marine $^{87}Sr/^{86}Sr$ record (Fig. 4), which is consistent with exceedingly high atmospheric CO_2 concentrations in the aftermath of the Marinoan glaciation (Hoffman et al., 1998; Kasemann et al., 2005). The resulting high rates of silicate weathering and nutrient delivery to the oceans (Higgins and Schrag, 2003) could have triggered high export production and burial of primary organic matter, driving an increase in atmospheric O_2.

During the transient phase of increasing M_{sulf}, pyrite weathering would have been a major sink for free oxygen in the atmosphere, preventing pO_2 from rising to higher levels. Once steady state in the exogenic sulfur cycle was reached, then this sink would have been balanced by sulfide burial (Holser et al., 1988), and O_2 would have

been free to accumulate in the atmosphere and oceans (unless consumed by some other sink). The combination of higher sulfate and oxygen concentrations would have then triggered a sharp increase in average $\Delta^{34}S$ (Canfield and Teske, 1996; Hurtgen et al., 2005), while the return to steady state conditions, during which time f_{pyr} remained high, would have led to gradually increasing $\delta^{34}S_{sulf}$ and $\delta^{34}S_{pyr}$ values. Based on the sulfur isotope compilation and our model results (Fig. 4), it appears as if this stage occurred, at least initially, shortly before the onset of the Shuram–Wonoka anomaly and Gaskiers glaciation, between 600 and 580 Ma.

As previously mentioned, the generation of such an extreme $\delta^{13}C$ anomaly, whether the result of the oxidation of an immense, dissolved organic carbon pool in the deep oceans (Rothman et al., 2003; Fike et al., 2006), the weathering of black shales (Workman et al., 2002), or the oxidation of a long-lived methane flux from sedimentary clathrate reservoirs (Pokrovskii et al., 2006), would have constituted an immense sink for free oxidants in the ocean. However, the perturbation apparently was not sufficient to prevent deep ocean oxygenation (Canfield et al., 2007) and the colonization of the Avalon continental slope by Ediacaran-type fauna by ca. 575 Ma (Narbonnne and Gehling, 2003).

7. Conclusions

A prolonged interval of unusually high $\Delta^{34}S$ values characterizes the late Neoproterozoic and early Paleozoic marine sulfate record. This interval of high $\delta^{34}S_{sulf}$ is best explained by a sharp increase in $\Delta^{34}S$, coupled to rapidly increasing marine sulfate concentrations, but decoupled from a compensatory decline in the fractional burial of sedimentary sulfides. A one dimensional model to simulate the growth the marine sulfate reservoir, in combination with a compilation of available $\Delta^{34}S$ data for the Ediacaran Period, suggests that sulfate concentrations increased to levels in excess of 48 mM ca. 600–580 Ma, prior to the onset of the Shuram–Wonoka negative $\delta^{13}C$ anomaly, the most extreme carbon isotope anomaly in Earth's history (Le Guerroué et al., 2006). This growth of the marine sulfate reservoir was accomplished by imbalanced weathering of continental sulfides, which inferentially required a certain critical threshold of free oxygen in the atmosphere. Thus, we postulate that both marine sulfate and atmospheric oxygen levels reached approximate Phanerozoic levels sometime in the middle Ediacaran Period, well in advance of the 575 Ma first appearance of Ediacaran-like fauna in deep water sediments in Newfoundland (Narbonnne and Gehling, 2003). The fact that there were sufficient oxidants available in the oceans to mineralize the immense influx of ^{13}C-depleted reduced carbon required to account for the Shuram–Wonoka anomaly is testament to high levels of marine $[SO_4]$ and pO_2 prior to ca. 580 Ma.

Acknowledgments

This study was supported by an NSF Post-Doctoral Research Fellowship to GPH while at LMTG-CNRS (Université Toulouse III). This paper has benefitted from discussions with Jochen Brocks, Don Canfield, Yves Goddéris, Paul Hoffman, Francis Macdonald, and Adam Maloof and the authors' participation in IGCP 512, as well as reviews by Andrew Hill and an anonymous referee.

References

Alt, J., 1995. Sulfur isotopic profile through the oceanic crust: sulfur mobility and seawater-crustal sulfur exchange during hydrothermal alteration. Geology 23, 585–588.

Amthor, J., Grotzinger, J., Schröder, S., Bowring, S., Ramezani, J., Martin, M., Matter, A., 2003. Extinction of *Cloudina* and *Namacalathus* at the Precambrian–Cambrian boundary in Oman. Geology 31, 431–434.

Anbar, A., Knoll, A., 2002. Proterozoic ocean chemistry and evolution: a bioinorganic bridge? Nature 297, 1137–1142.

Arnold, G., Anbar, A., Barling, J., Lyons, T., 2004. Molybdenum isotope evidence for widespread anoxia in mid-Proterozoic oceans. Science 304, 87–90.

Berner, R., 2001. Modeling atmospheric O_2 over Phanerozoic time. Geochimica et Cosmochimica Acta 65, 685–694.

Berner, R., 2004. A model for calcium, magnesium and sulfate in seawater over Phanerozoic time. American Journal of Science 304, 438–453.

Burdett, J., Arthur, M., Richardson, M., 1989. A Neogene seawater sulfur isotope age curve from calcareous pelagic microfossils. Earth and Planetary Science Letters 94.

Canfield, D., 1998. A new model for Proterozoic ocean chemistry. Nature 396, 450–453.

Canfield, D., 2004. The evolution of the earth surface sulfur reservoir. American Journal of Science 304, 839–861.

Canfield, D., 2005. The early history of atmospheric oxygen. Annual Review of Earth and Planetary Sciences 33, 1–36.

Canfield, D., Teske, A., 1996. Late Proterozoic rise in atmospheric oxygen concentration inferred from phylogenetic and sulphur-isotope studies. Nature 382, 127–132.

Canfield, D., Thamdrup, B., 1994. The production of ^{34}S-depleted sulfide during bacterial disproportionation of elemental sulfur. Science 266, 1973–1975.

Canfield, D., Raiswell, R., Westrich, J., Reaves, C., Berner, R., 1986. The use of chromium reduction in the analysis of reduced inorganic sulfur in sediments and shales. Chemical Geology 54, 149–155.

Canfield, D., Poulton, S., Narbonne, G., 2007. Late-Neoproterozoic deep-ocean oxygenation and the rise of animal life. Science 315, 92–95.

Catling, D., Claire, M., 2005. How Earth's atmosphere evolved to an oxic state: a status report. Earth and Planetary Science Letters 237, 1–20.

Claypool, G., Holser, W., Kaplan, I., Sakai, H., Zak, I., 1980. The age curves of sulfur and oxygen isotopes in marine sulfate and their mutual interpretation. Chemical Geology 288, 199–260.

Condon, D., Zhu, M., Bowring, S., Jin, Y., Wang, W., Yang, A., 2005. From the Marinoan glaciation to the oldest bilaterians: U–Pb ages from the Doushantuo Formation, China. Science 308, 95–98.

Derry, L., Brasier, M., Corfield, R., Rozanov, A., Zhuravlev, A., 1994. Sr and C isotopes in Lower Cambrian carbonates from the Siberian craton: a paleoenvironmental record during the "Cambrian explosion". Earth and Planetary Science Letters 128, 671–681.

Fike, D., Grotzinger, J., Pratt, L., Summons, R., 2006. Oxidation of the Ediacaran Ocean. Nature 444, 744–747.

Goldberg, T., Poulton, S., Strauss, H., 2005. Sulphur and oxygen isotope signatures of late Neoproterozoic to early Cambrian sulphate, Yangtze Platform, China: diagenetic constraints and seawater evolution. Precambrian Research 137, 223–241.

Gorjan, P., Veevers, J., Walter, M., 2000. Neoproterozoic sulfur-isotope variation in Australia and global implications. Precambrian Research 100, 151–179.

Grantham, P., Lijmbach, G., Posthuma, J., Clarke, M., Willink, R., 1988. Origin of crude oils in Oman. Journal of Petroleum Geology 11, 61–80.

Grotzinger, J., Kasting, J., 1993. New constraints on Precambrian ocean composition. Journal of Geology 101, 235–243.

Habicht, K., Canfield, D., 2001. Isotope fractionation by sulfate-reducing natural populations and the isotopic composition of sulfide in marine sediments. Geology 29, 555–558.

Habicht, K., Cade, M., Thamdrup, B., Berg, P., Canfield, D., 2002. Calibration of sulfate levels in the Archean ocean. Science 298, 2372–2374.

Halverson, G., 2006. A Neoproterozoic chronology. In: Xiao, S., Kaufman, A. (Eds.), Neoproterozoic Geobiology and Paleobiology. Springer, Dordrecht, the Netherlands, pp. 231–271. Vol. 27 of Topics in Geobiology.

Halverson, G., Hoffman, P., Schrag, D., Maloof, A., Rice, A., 2005. Towards a Neoproterozoic composite carbon isotope record. Geological Society of America Bulletin 117, 1181–1207.

Halverson, G., Dudas, F., Maloof, A., Bowring, S., in press. Evolution of the $^{87}Sr/^{86}Sr$ composition of Neoproterozoic seawater. Palaeogeography, Palaeoclimatology, Palaeoecology.

Hayes, J., Strauss, H., Kaufman, A., 1999. The abundance of ^{13}C in marine organic carbon and isotopic fractionation in the global biogeochemical cycle of carbon during the past 800 Ma. Chemical Geology 161, 103–125.

Higgins, J., Schrag, D., 2003. Aftermath of a snowball Earth. Geochemistry, Geophysics, Geosystems 431. doi:10.1029/2002GC000403.

Hoffman, P., Kaufman, A., Halverson, G., Schrag, D., 1998. A Neoproterozoic snowball Earth. Science 281, 1342–1346.

Hoffmann, K., Condon, D., Bowring, S., Crowley, J., 2004. A U–Pb zircon date from the Neoproterozoic Ghaub Formation, Namibia: constraints on Marinoan glaciation. Geology 32 (9), 817–820.

Hoffman, P., Halverson, G., Domack, E., Husson, J., Higgins, J., Schrag, D., 2007. Are basal Ediacaran (635 Ma post-glacial "cap dolostones" diachronous? Earth and Planetary Science Letters 258, 114–131.

Holser, W., 1977. Catastrophic chemical events in the history of the ocean. Nature 267, 403–408.

Holser, W., Kaplan, I., 1966. Isotope geochemistry of sedimentary sulfates. Chemical Geology 1, 93–135.

Holser, W., Schidlowski, M., Mackenzie, F., Maynard, J., 1988. Geochemical cycles of carbon and sulfur. In: Gregory, C., Garrels, R., Mackenzie, F., Maynard, J. (Eds.), Chemical cycles in the evolution of the Earth. Wiley, John & Sons, pp. 105–173.

Holser, W., Maynard, J., Cruikshank, K., 1989. In: Brimblecombe, P., Yu, A. (Eds.), Evolution of the global biogeochemical sulfur cycle. Wiley, New York, NY, pp. 21–56.

Horita, J., Zimmerman, H., Holland, H., 2002. Chemical evolution of seawater during the Phanerozoic: implications from the record of marine evaporites. Geochimica et Cosmochimica Acta 66, 3733–3756.

Hurtgen, M., Arthur, M., Suits, N., Kaufman, A., 2002. The sulfur isotopic composition of Neoproterozoic seawater sulfate: implications for snowball Earth? Earth and Planetary Science Letters 203, 413–429.

Hurtgen, M., Arthur, M., Prave, A., 2004. The sulfur isotopic composition of carbonate-associated sulfate in Mesoto Neoproterozoic carbonates from Death Valley, CA. In: Amend, J., Edwards, K., Lyons, T. (Eds.), Sulfur Biogeochemistry—Past and Present. Geological Society of America Special Paper, vol. 379. Geological Society of America, pp. 177–194.

Hurtgen, M.T., Arthur, M.A., Halverson, G.P., 2005. Neoproterozoic sulfur isotopes, the evolution of microbial sulfur species, and the burial efficiency of sulfide as sedimentary sulfide. Geology 33, 41–44.

Hurtgen, M., Halverson, G., Arthur, M., Hoffman, P., 2006. Sulfur cycing in the aftermath of a Neoproterozoic (Marinoan) snowball glaciation: evidence for a syn-glacial sulfidic deep ocean. Earth and Planetary Science Letters 245, 551–570.

Hyde, W., Crowley, T., Baum, S., Peltier, W., 2000. Neoproterozoic 'snowball Earth' simulations with a coupled climate/ice-sheet model. Nature 405, 425–429.

Johnston, D., Wing, B., Farquhar, J., Kaufman, A., Strauss, H., Lyons, T., Kah, L., Canfield, D., 2005. Active microbial sulfur disproportionation in the Mesoproterozoic. Science 310, 1477–1479.

Jørgensen, B., 1990. A thiosulfate shunt in the sulfur cycle of marine sediments. Science 249, 152–154.

Kah, L., Lyons, T., Frank, T., 2004. Low marine sulphate and protracted oxygenation of the Proterozoic biosphere. Nature 431, 834–838.

Kampschulte, A., Strauss, H., 2004. The sulfur isotopic evolution of Phanerozoic seawater based on the analysis of structurally substituted sulfate in carbonates. Chemical Geology 204, 255–286.

Kasemann, S., Hawkesworth, C., Prave, A., Fallick, A., Pearson, P., 2005. Boron and calcium isotope composition in Neoproterozoic carbonate rocks from Namibia: evidence for extreme environmental change. Earth and Planetary Science Letters 231, 73–86.

Kaufman, A., Corsetti, F., Varni, M., 2007. The effect of rising atmospheric oxygen on carbon and sulfur isotope anomalies in the Neoproterozoic Johnnie Formation, Death Valley, USA. Chemical Geology 237, 47–63.

Knoll, A., 2003. Life on a Young Planet. Princeton University Press, Princeton.

Le Guerroué, E., Allen, P., Cozzi, A., 2006. Chemostratigraphic and sedimentological framework of the largest negative carbon isotopic excursion in Earth history: the Neoproterozoic Shuram Formation (Nafun Group, Oman). Precambrian Research 146, 68–92.

Logan, G.A., Hayes, J.M., Hieshima, G.B., Summons, R., 1995. Terminal Proterozoic reorganization of biogeochemical cycles. Nature 376, 53–56.

Lyons, T., 1997. Sulfur isotopic trends and pathways of iron sulfide formation in upper Holocene sediments of the anoxic Black Sea. Geochimica et Cosmochimica Acta 61, 3367–3382.

Narbonnne, G., Gehling, J., 2003. Life after snowball: the oldest complex Ediacaran fossils. Geology 31, 27–30.

Neretin, L., Böttcher, M., Grinenko, V., 2003. Sulfur isotope geochemistry of the Black Sea water column. Chemical Geology 200, 59–69.

Newton, R., Pevitt, E., Wignall, P., Bottrell, S., 2004. Large shifts in the isotopic composition of seawater sulphate across the Permo-Triassic boundary in northern Italy. Earth and Planetary Science Letters 218, 331–345.

Paytan, A., Kastner, M., Campbell, D., Thiemens, M., 1998. Sulfur isotopic composition of Cenozoic seawater sulfate. Science 282, 1459–1462.

Petsch, S., Berner, R., 1998. Coupling the geochemical cycles of C, P, Fe, and S: the effect on atmospheric O_2 and the isotopic records of carbon and sulfur. Americal Journal of Science 298, 246–262.

Pisarchik, Y., Golubchina, M., Toksubayev, A., 1977. Isotopic composition of sulfur in calcium sulfates from the upper Lena Formation (Siberian Platform). Geochemistry International 14, 182–185.

Pokrovskii, B., Melezhik, V., Bujakaite, M., 2006. Carbon, oxygen, strontium, and sulfur isotopic compositions in late Precambrian rocks of the Patom Complex, central Siberia: Communication 2. Nature of carbonates with ultralow and ultrahigh $\delta^{13}C$ values. Lithology and Mineral Resources 41, 576–587.

Ridgwell, A., Zeebe, R.E., 2005. The role of the global carbonate cycle in the regulation and evolution of the Earth system. Earth and Planetary Science Letters 234, 299–315.

Ross, G., Bloch, J., Krause, H., 1995. Neoproterozoic strata of the southern Canadian Cordillera and the isotopic evolution of seawater sulfate. Precambrian Research 73, 71–99.

Rothman, D., Hayes, J., Summons, R., 2003. Dynamics of the Neoproterozoic carbon cycle. Proceedings of the National Academy of Sciences 100 (14), 124–129.

Runnegar, B., 1991. Precambrian oxygen levels estimated from the biochemistry and physiology of early eukaryotes. Palaeogeography, Palaeoclimatology, Palaeoecology 97, 97–111.

Saltzman, M., 2005. Phosphorus, nitrogen, and the redox evolution of the Paleozoic oceans. Geology 33, 573–576.

Schröder, S., Schreiber, B., Amthor, J., Matter, A., 2003. A depositional model for the terminal Neoproterozoic–Eearly Cambrian Ara Group evaporites in south Oman. Sedimentology 50, 879–898.

Schröder, S., Schreiber, B.C., Amthor, J., Matter, J., 2004. Stratigraphy and environmental conditions of the terminal Neoproterozoic–Cambrian Period in Oman: evidence from sulphur isotopes. Journal of the Geological Society of London 161, 489–499.

Shen, Y., Knoll, A., Walter, M., 2003. Evidence for low sulphate and anoxia in a mid-Proterozoic marine basin. Nature 423, 632–635.

Shields, G., Strauss, H., Howe, S., Siegmund, H., 1999. Sulphur isotope compositions of sedimentary phosphorites from the basal Cambrian of China: implications for Neoproterozoic–Cambrian biogeochemical cycling. Journal of the Geological Society of London 156, 943–955.

Shields, G., Kimura, H., Yang, J., Gammon, P., 2004. Sulphur isotopic evolution of Neoproterozoic–Cambrian seawater: new francolite-bound sulphate $\delta^{34}S$ data and critical appraisal of the existing record. Chemical Geology 204, 163–182.

Strauss, H., 1993. The sulfur isotopic record of Precambrian sulfates: new data and a critical evalution of the existing record. Precambrian Research 63, 225–246.

Strauss, H., 1997. The isotope composition of sedimentary sulfur through time. Palaeogeography, Palaeoclimatology, Palaeoecology 132, 97–118.

Strauss, H., Banerjee, D., Kuman, V., 2001. The sulfur isotopic composition of Neoproterozoic to early Cambrian seawater-evidence from the cyclic Hasneran evaporites, NW India. Chemical Geology 175, 17–28.

Trindade, R., Font, E., D'Agrella-Filho, M., Nogueira, A., Riccomini, C., 2003. Low-latitude and multiple geomagnetic reversals in the Neoproterozoic Puga cap carbonate, Amazon craton. Terra Nova 15 (6), 441–446.

Wang, Z., Chu, X., 1991. Barite and witherite deposits in lower Cambrian shales of South China: stratigraphic distribution and geochemical characterization. Economic Geology 86, 354–363.

Workman, R., Grotzinger, J., Hart, S., 2002. Constraints on Neoproterozoic ocean chemistry from $\delta^{13}C$ and $\delta^{11}B$ analyses of carbonates from the Witvlei and Nama Groups. Geochimica et Cosmochimica Acta 16 (15A), A847.